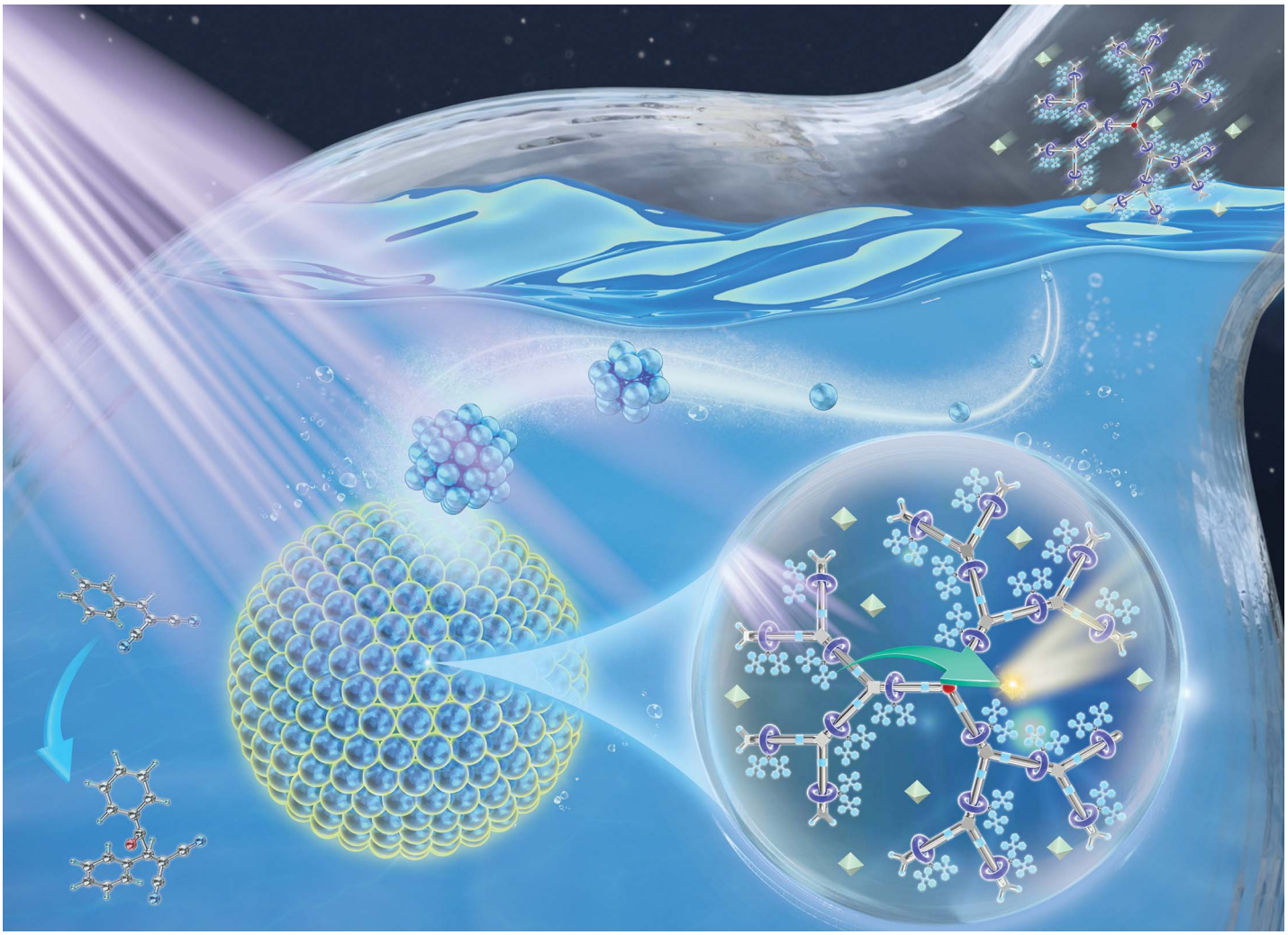

Showcasing research from Professor Hai-Bo Yang's laboratory, School of Chemistry and Molecular Engineering, East China Normal University, Shanghai 200062, China.

Artificial light harvesting systems based on novel AIEgen-branched rotaxane dendrimers for photocatalyzed functionalization of C–H bonds

A novel type of AIEgen-branched rotaxane dendrimers with up to 42 TPE units precisely distributed with the dendrimer skeletons have been successfully synthesized, based on which artificial light harvesting systems are further constructed through efficient FRET process and display interesting generation-dependent photocatalytic performances in the functionalization of C-H bonds.

Image reproduced by permission of Hai-Bo Yang from *Chem. Sci.,* 2025, **16**, 5786.

As featured in:

See Xu-Qing Wang, Hai-Bo Yang *et al.*, *Chem. Sci.,* 2025, **16**, 5786.

ROYAL SOCIETY OF CHEMISTRY

15 YEARS ANNIVERSARY

rsc.li/chemical-science

Registered charity number: 207890

Chemical Science

ROYAL SOCIETY OF CHEMISTRY

EDGE ARTICLE

View Article Online
View Journal | View Issue

Cite this: *Chem. Sci.*, 2025, **16**, 5786

All publication charges for this article have been paid for by the Royal Society of Chemistry

Received 10th January 2025
Accepted 1st March 2025

DOI: 10.1039/d5sc00224a

rsc.li/chemical-science

Artificial light harvesting systems based on novel AIEgen-branched rotaxane dendrimers for photocatalyzed functionalization of C–H bonds†

Xiao-Qin Xu,[a] Yi-Ru Song,[a] Jiang-Han Cao,[a] Wei-Jian Li,[a] Yu Zhu,[a] Dan-Yang Zhang,[a] Wei Wang,[a] Xu-Qing Wang*[d] and Hai-Bo Yang *[abc]

Aiming at the construction of novel luminescent materials for practical use, a new type of AIEgen-branched rotaxane dendrimer with up to 42 TPE units precisely distributed with dendrimer skeletons was successfully synthesized. Attributed to such high-density topological arrangements of AIEgens, these novel rotaxane-branched dendrimers revealed interesting generation-dependent AIE behaviors. Moreover, taking advantage of the efficient Förster resonance energy transfer (FRET) process, novel artificial light-harvesting systems (LHSs) were successfully constructed by the employment of ESY as energy acceptors, which revealed significantly enhanced photocatalytic performances in the functionalization of C–H bonds along with an increase in dendrimer generation, thus indicating an impressive generation effect.

Introduction

Photosynthesis is the basis for the survival and development of life in nature.[1] Green plants harvest light through a pigment-antenna protein complex containing a large number of tightly arranged chlorophyll molecules to energy acceptor carotenoids, which is converted into chemical energy *via* continuous exciton/energy migration.[2] Chemists have tried to design artificial light-harvesting systems (LHSs) for a long time by mimicking this natural photosynthetic process in order to develop a sustainable clean energy source.[3] In recent years, various systems based on porphyrin arrays,[4] dendrimers,[5] organogels,[6] metal–organic frameworks,[7] polymers,[8] organic nanocrystals[9] and others[10] have been developed for the construction of artificial LHSs. A common approach is to mimic the natural light-harvesting process between the donor and acceptor through the Förster resonance energy transfer (FRET) process.[11] Notably, the construction of efficient artificial LHSs requires a high ratio of energy donors to acceptors and a tight packing degree of energy donors.[12] However, this tight arrangement usually results in the aggregation-caused quenching (ACQ) effect of the donor's fluorescence, which might further lead to reduced efficiency.[13] Fortunately, the aggregation-induced emission (AIE) effect coined by Tang *et al.* in 2001 effectively made up for this deficiency.[14] Luminogens with a typical AIE effect, often referred to as AIEgens, have restricted intramolecular motions (RIMs) in the aggregated state, which effectively blocks the non-radiative energy dissipation pathway, thus leading to enhanced emissions and other intriguing properties.[15]

Notably, AIE-active dendrimers have recently received extensive attention, attributed to their great potential in the construction of novel luminescent materials. Compared with other types of well-investigated AIE-active polymers, AIE-active dendrimers have unique star-shaped hyperbranched structures and well-defined topological arrangements of AIEgens, which could serve as ideal platforms for the rational design and construction of novel artificial LHSs.[16] However, thus far, most of the reported AIE-active dendrimers only focus on AIEgen-cored and AIEgen-terminated dendrimers owing to the lack of appropriate AIEgen building blocks with suitable functional groups for the growth of dendrimers, thus making the synthesis of AIEgen-branched dendrimers quite difficult.[17] Notably, the introduction of AIEgen units on the branches of AIEgen-branched dendrimers' skeleton would provide promising platforms for the construction of novel artificial LHSs with high fluorescence brightness and high donor density, which is of great importance. In 2021, our group introduced the TPE unit, the most classical AIEgen, as a stopper of the key [2]rotaxane building block, leading to the successful synthesis of a new type of rotaxane-branched dendrimer with AIEgens located on branches for the first time through a controllable divergent approach.[18] To further enrich the family of AIEgen-branched

[a]*Shanghai Key Laboratory of Green Chemistry and Chemical Processes, State Key Laboratory of Petroleum Molecular and Process Engineering, School of Chemistry and Molecular Engineering, East China Normal University, Shanghai 200062, China. E-mail: hbyang@chem.ecnu.edu.cn*

[b]*Shanghai Center of Brain-inspired Intelligent Materials and Devices, East China Normal University, Shanghai 200241, China*

[c]*Shanghai Frontiers Science Center of Molecule Intelligent Syntheses, East China Normal University, Shanghai 200062, China*

[d]*School of Chemical and Environmental Engineering and Shanghai Engineering Research Center of Green Fluoropharmaceutical Technology, Shanghai Institute of Technology, Shanghai 201418, China. E-mail: xqwang@sit.edu.cn*

† Electronic supplementary information (ESI) available. See DOI: https://doi.org/10.1039/d5sc00224a

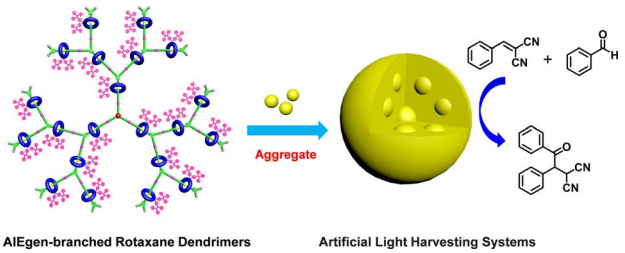

Fig. 1 The design and synthesis of a new type of AIEgen-branched rotaxane dendrimer for the construction of novel artificial light harvesting systems that display excellent photocatalytic performances in the functionalization of C–H bonds.

rotaxane dendrimers, the introduction of AIEgens units into the wheel component of the rotaxane branches with the dendrimer skeleton will be of great interest, but more challenging. On the one hand, in this newly-proposed AIEgen-branched rotaxane dendrimer, AIEgens units can exhibit more precise topological arrangements and move along the axle component in response to additional stimuli, which is expected to afford superior LHS characteristics. On the other hand, compared with rotaxane dendrimers with AIEgens units modified on the axle component, AIEgens units modified on the wheel component would lead to a more significant steric hindrance effect due to more crowded distributions, which might significantly improve their AIE performances. Based on these advantages, it will be of great importance to construct such novel AIEgen-branched rotaxane dendrimers and further investigate their light-harvesting performances, as well as related applications.

Herein, based on our on-going research interest in mechanically interlocked molecules (MIMs),[19] particularly rotaxane dendrimers,[20] a novel class of AIEgen-branched rotaxane dendrimers with up to 42 AIEgens units on their branches has been designed and synthesized for the first time by introducing two TPE units into the wheel components of the key [2]rotaxane building block. Such a high AIEgens density would be of crucial importance in improving the light harvesting efficiency. Moreover, the dendrimer skeleton will exert a more significant steric hindrance effect on the AIEgens units, thereby enhancing the performance of AIE. Notably, the introduction of the urea recognition sites can endow the resulting AIEgen-branched rotaxane dendrimers with interesting dynamic AIE behavior. More importantly, by doping the fluorescent dye ESY upon the aggregate, these AIE-active rotaxane-branched dendrimers can be further used for the construction of novel artificial LHSs, which exhibit impressive catalytic performances in the functionalization of inert C–H bonds through typical hydrogen-atom transfer (HAT) processes (Fig. 1).

Results and discussion

Design, synthesis, and characterization of novel AIEgen-branched rotaxane dendrimers

In this study, a novel functionalized [2]rotaxane **TPE-R** was designed and synthesized by the formation of a host–guest complex between the pillar[5]arene macrocycle and long-chain alkanes. In this [2]rotaxane building block, two TPE units were attached to the pillar[5]arene macrocycle as the wheel component. In addition, TIPS-protected alkynes were introduced into the axle component as the stopper, which can be converted into the alkyne group under mild conditions and serve as subsequent dendrimer growth sites. Notably, the introduction of the urea moiety into the axle component as a recognition site not only contributes to the formation of [2]rotaxanes through enhanced host–guest complexing, but also allows the wheel component to undergo translational movement along the axle component, thus possibly endowing the targeted AIEgen-branched rotaxane dendrimers with interesting stimuli-responsive properties. On the basis of such design strategy, the [2]rotaxane building block **TPE-R** was successfully prepared by a threading-followed-by-stoppering strategy with a yield of 70% on a gram scale (ESI, Scheme S1†), which was fully characterized by various techniques including 1-D multinuclear (^{1}H, ^{13}C, and ^{31}P), 2-D NMR (^{1}H–^{1}H COSY, ROESY) spectroscopy, and ESI-TOF-MS analysis (Fig. S1–S9†).

After the successful and efficient synthesis of the key AIEgen-based [2]rotaxane **TPE-R** building block, 1,3,5-triethynylbenzene was selected as the core unit of the rotaxane-branched dendrimer. The efficient construction of the targeted rotaxane-branched dendrimers with a high density of AIEgens on the skeleton was realized by the stepwise controlled divergent strategy. As shown in Fig. 2a, with CuI as the catalyst, [2]rotaxane **TPE-R** reacted with the 1,3,5-triethynylbenzene core unit to produce the first generation rotaxane-branched dendrimer **TPE-G1** with a yield of 88%. It contains three rotaxane units with two TPE units distributed on each branch. Subsequently, at room temperature, the deprotected intermediate **TPE-G1-YNE** was obtained by adding tetrabutylammonium fluoride trihydrate ($Bu_4NF\cdot 3H_2O$) to the tetrahydrofuran solution of **TPE-G1**. After the removal of the protective groups, six alkynyl reaction growth sites in the intermediate were exposed, which further reacted with **TPE-R** to obtain the second-generation rotaxane-branched dendrimer **TPE-G2** with nine AIEgen-based [2]rotaxane units and 18 TPE units on the branches in a yield of 72% (Fig. 2b). Based on the above iterative deprotection-coupling growth process, the third-generation rotaxane-branched dendrimer **TPE-G3** with a high density of AIEgens was then successfully synthesized in 78% yield. Impressively, **TPE-G3** contains 21 rotaxane units and 42 TPE units on the branches.

The structures of the synthesized AIEgen-branched rotaxane dendrimers **TPE-G*n*** (n = 1, 2, and 3) were first characterized by ^{1}H and ^{31}P NMR spectroscopy. As shown in Fig. S19,† a set of sharp and regular signals were observed in the ^{1}H NMR spectra of **TPE-G*n*** (n = 1, 2, and 3), which initially indicated that the obtained rotaxane-branched dendrimers **TPE-G*n*** (n = 1, 2, and 3) were discrete structures, excluding the possible formation of polymers or oligomers. Moreover, no proton peaks attributed to the terminal alkyne were observed at the chemical shifts around 4.0 ppm, indicating that all the terminal alkynes had been completely reacted. Thus, the obtained rotaxane-branched dendrimers had no structural defects. More importantly, the

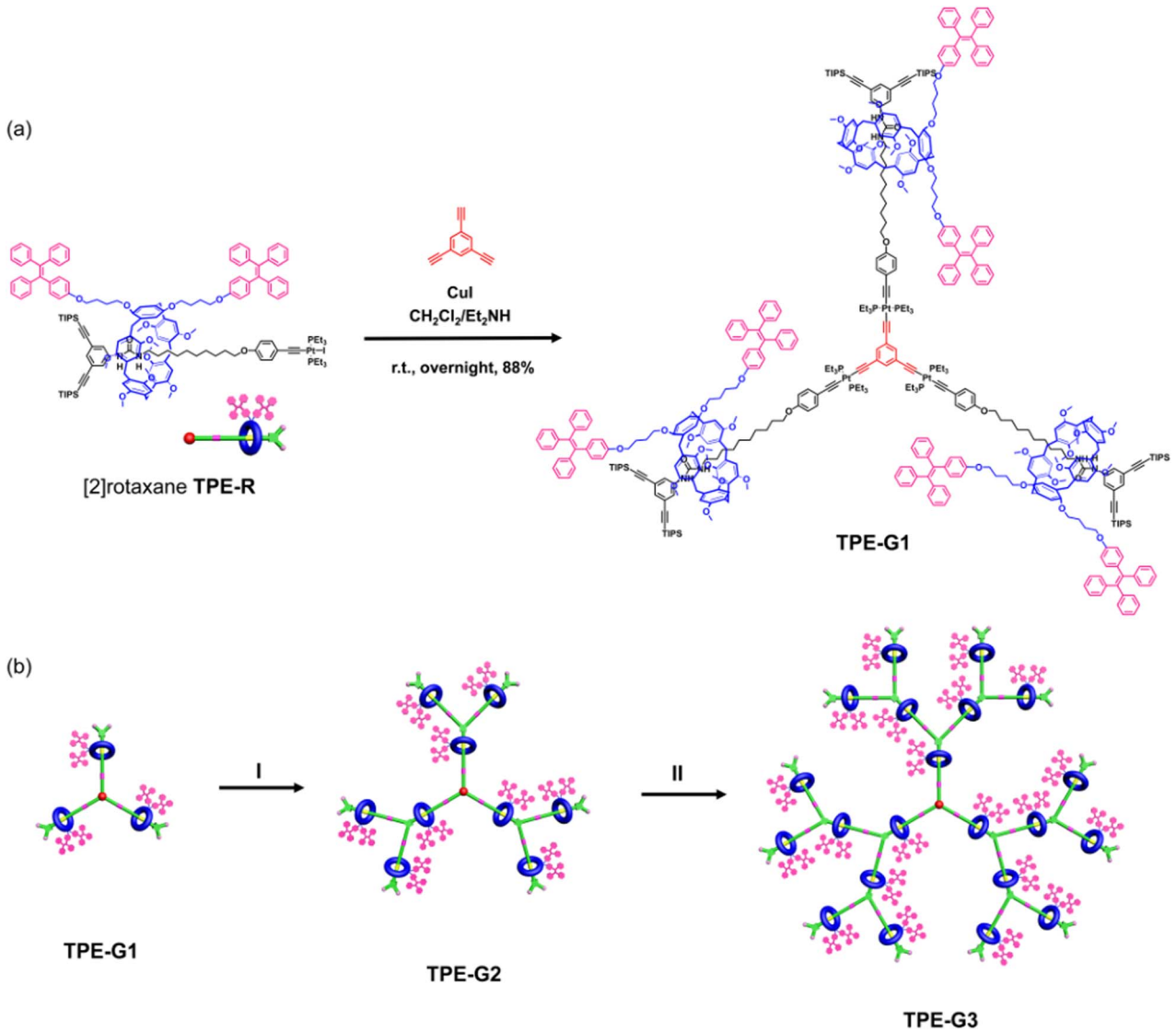

Fig. 2 (a) Synthesis of the TPE-branched rotaxane dendrimer **TPE-G1** *via* a CuI-catalyzed coupling reaction of **TPE-R** and 1,3,5-triethynylbenzene. (b) Representation of a controllable divergent strategy for the synthesis of the AIEgen-branched rotaxane dendrimers **TPE-G2** and **TPE-G3**. Reaction conditions: (I): (a) $Bu_4NF \cdot 3H_2O$, THF, rt, and 2 h; (b) **TPE-R**, CuI, DCM/Et_2NH, rt, overnight, and 72%; (II): (a) $Bu_4NF \cdot 3H_2O$, THF, rt, and 2 h; (b) **TPE-R**, CuI, DCM/Et_2NH, rt, overnight, and 78%.

presence of the characteristic signals of the rotaxane units at the chemical shifts below 0.0 ppm revealed that the interlocked structures were not destroyed during the growth of the rotaxane-branched dendrimers. Notably, for higher-generation rotaxane-branched dendrimers, several new peaks attributed to the threaded structures were observed, indicating that the rotaxane subunits located on different branches were nonequivalent. In addition, as shown in Fig. S20,† single and sharp characteristic peaks were observed in all ^{31}P NMR spectra, indicating that all the rotaxane-branched dendrimers have highly symmetric skeletons. Compared to the [2]rotaxane building block **TPE-R**, the chemical shifts of the PEt_3 ligands belonging to **TPE-G*n*** (n = 1, 2, and 3) displayed downfield shifts, which further illustrated the formation of double-substituted platinum-acetylide bonds in the preparation of the AIEgen-branched rotaxane dendrimers by coupling reaction. Similar with that in the ^1H NMR spectra, different chemical shifts of phosphine ligands were also found for different generations, along with the growth of the AIEgen-branched rotaxane dendrimers, again indicating the nonequivalent chemical environments of different generations. Therefore, the successful synthesis of targeted rotaxane-branched dendrimers **TPE-G*n*** (n = 1, 2, and 3) were confirmed by 1-D NMR analysis.

Next, the AIEgen-branched rotaxane dendrimers **TPE-G*n*** (n = 1, 2, and 3) were further characterized by mass spectrometry (MALDI-TOF-MS). In the MALDI-TOF-MS spectrum of **TPE-G1**, the main characteristic peak at m/z = 8282.2 was observed, which was attributed to the [**TPE-G1** + H]$^+$ ion peak and is fully consistent with the theoretical value (m/z = 8282.9). Thus, the successful preparation of **TPE-G1** was directly confirmed

(Fig. S21†). Furthermore, for **TPE-G2**, the main characteristic peak was observed at $m/z = 23\,639.8$, which was ascribed to the $[\textbf{TPE-G2}]^+$ ion peak and agreed well with the theoretical value ($m/z = 23\,639.3$), indicating the successful synthesis of **TPE-G2** (Fig. S22†). However, due to the high molecular weight ($M = 54\,291$ Da) and low ionization efficiency, the expected MS analysis results of **TPE-G3** could not been obtained even after successive attempts. Therefore, the monodispersity of these AIEgen-branched rotaxane dendrimers was then evaluated by GPC analysis. As shown in Fig. S23–S25,† all these rotaxane-branched dendrimers **TPE-G*n*** (n = 1, 2, and 3) showed a single peak with narrow distribution of the number-averaged molecular weight (M_n), and their polydispersity index (PDI) was 1.02 (**TPE-G1**), 1.02 (**TPE-G2**) and 1.05 (**TPE-G3**), respectively. These results clearly suggest that the targeted monodisperse rotaxane-branched dendrimers **TPE-G*n*** (n = 1, 2, and 3) have been successfully synthesized.

In addition, the monodispersity of these rotaxane-branched dendrimers was further evaluated by two-dimensional diffusion-ordered spectroscopy (2-D DOSY). As revealed by all the DOSY spectra, only one set of signals corresponding to a single species was found. More importantly, the diffusion coefficient (D) significantly decreased with the generation increase of AIEgen-branched rotaxane dendrimers (2.19×10^{-10} m^2 s^{-1} for **TPE-G1**, 1.32×10^{-10} m^2 s^{-1} for **TPE-G2**, and 7.41×10^{-11} m^2 s^{-1} for **TPE-G3**), which further proved that the sizes of the obtained rotaxane-branched dendrimers gradually increase (Fig. S26–S28†). To further confirm the formation of rotaxane-branched dendrimers, dynamic light scattering (DLS) was then used to characterize the size of the resulting rotaxane-branched dendrimers **TPE-G*n*** (n = 1, 2, and 3) (Fig. S60–S62†). All the signals were observed as a single, regular peak pattern and the average hydrodynamic sizes (D_h) of the rotaxane-branched dendrimer were 3.6 ± 0.1 nm (**TPE-G1**), 5.6 ± 0.2 nm (**TPE-G2**), and 8.7 ± 0.5 nm (**TPE-G3**), which were in agreement with the results obtained by the 2-D DOSY NMR study. The morphologies of the synthesized AIEgen-branched rotaxane dendrimers **TPE-G*n*** (n = 1, 2, and 3) were further characterized using atomic force microscopy (AFM) measurements. As shown in Fig. S29,† the average heights of these rotaxane dendrimers progressively increased with the growth of the dendrimer generations from 4.1 ± 0.2 nm (**TPE-G1**) to 5.9 ± 0.1 nm (**TPE-G2**), and finally to 8.8 ± 0.3 nm (**TPE-G3**). This gradual increase in height provides additional evidence for the successful synthesis of the targeted AIEgen-branched rotaxane dendrimers **TPE-G*n*** (n = 1, 2, and 3).

Notably, due to the presence of the urea moiety as stimuli-responsive sites in each rotaxane branch of these resultant rotaxane-branched dendrimers, their dynamic behaviors under external stimuli were studied. As revealed by the ^{1}H NMR spectra shown in Fig. S30–S33,† by adding 5.0 equiv. CF_3COO^- (bis(triphenylphosphine)iminium trifluoroacetate) to the THF-d_8 solution of [2] rotaxane **TPE-R** or rotaxane dendrimers **TPE-G*n*** (n = 1, 2, and 3), the proton signals on the urea moiety (Hu_1 and Hu_2) displayed remarkable downfield shifts, while the signals of H_2 and H_3 exhibited obvious upfield shifts, indicating that the pillar[5]arene wheels moved from the urea moiety to the neutral alkyl chain station due to the formation of hydrogen bonding complexes between the trifluoroacetate anion and the urea moiety. Moreover, the further addition of NaTFPB to remove the trifluoroacetate anion as the CF_3COONa precipitate led to almost the same spectra as that of the original states, thus suggesting the movement of the pillar[5]arene wheels back to the original urea station. According to these results, these AIEgen-branched rotaxane dendrimers reveal interesting stimuli-responsive features, which makes them attractive platforms for the construction of smart luminescent materials.

Light harvesting systems based on novel AIEgen-branched rotaxane dendrimers

With the targeted AIEgen-branched rotaxane dendrimers **TPE-G*n*** (n = 1, 2, and 3) in hand, we then evaluated their AIE behaviors originated from the high density of TPE units distributed in their skeletons. In this study, CH_2Cl_2 and acetonitrile were selected as good and poor solvents, respectively. The characteristic absorption bands at around 292 nm and 345 nm were observed in the absorption spectra of **TPE-G*n*** (n = 1, 2, and 3), which were attributed to the pillar[5]arene moieties and TPE moieties, respectively (Fig. S34–S36†). When a certain fraction of acetonitrile (f_a) was added, significant changes in absorption spectra were observed, indicating the aggregation of the rotaxane-branched dendrimers. In addition, fluorescence spectra showed that in pure CH_2Cl_2 solution, all the rotaxane-branched dendrimers **TPE-G*n*** (n = 1, 2, and 3) displayed very weak fluorescence. However, when the fraction of the poor solvent acetonitrile was gradually increased, the emission intensity of **TPE-G*n*** (n = 1, 2, and 3) was significantly enhanced, showing a typical AIE behavior (Fig. 3a–c). For instance, when f_a was gradually increased to 70%, the emission intensity was almost constant. Further increasing the f_a values to 75% and above, a rapid enhancement of the emission intensity was observed. When 98% acetonitrile was added, the fluorescence intensity of **TPE-G1** reached the maximum, and the maximum emission wavelength was maintained at 480 nm. These observations suggested that different acetonitrile fractions can initiate the AIE effect of rotaxane-branched dendrimers. In addition, the absorption spectra showed a slight red-shift, indicating that there might be interactions between the rotaxane-branched dendrimers as the degree of aggregation increases.

For the rotaxane-branched dendrimer **TPE-G2**, the fluorescence emission intensity evidently began to enhance when the f_a was 60%. Meanwhile, in the case of the rotaxane-branched dendrimer **TPE-G3**, its fluorescence emission intensity started to be enhanced when f_a was 50%, indicating an obvious generation-dependent AIE behaviors of these rotaxane-branched dendrimers. However, for [2]rotaxane **TPE-R**, even under the condition of f_a at 98%, only very weak fluorescence was observed (Fig. S37†). This suggests that the dendritic skeleton of the rotaxane-branched dendrimers can significantly boost the AIE performances. Notably, with the increase of the generation, the enhancement of fluorescence intensity gradually decreased from 4.1-fold for **TPE-G1** to 3.0-fold for **TPE-G2**,

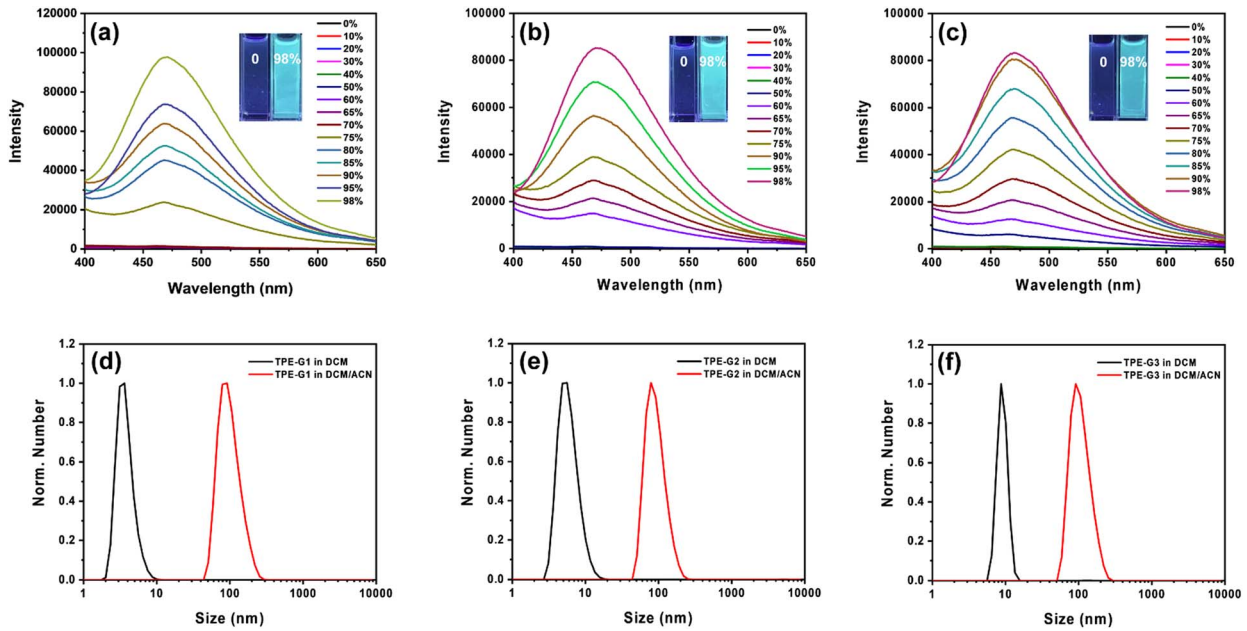

Fig. 3 AIE behaviors of the AIEgen-branched rotaxane dendrimers **TPE-G*n*** ($n = 1$, 2, and 3). Fluorescence spectra of **TPE-G1** (a), **TPE-G2** (b), and **TPE-G3** (c) in DCM/ACN with various ACN fractions ([TPE units] = 50 μM, $\lambda_{ex} = 345$ nm), inset: photographs of **TPE-G*n*** ($n = 1$, 2, and 3) in DCM/ACN with 0% (left) and 98% (right) ACN fractions upon UV excitation ($\lambda_{ex} = 365$ nm); DLS data for **TPE-G1** (d), **TPE-G2** (e), and **TPE-G3** (f) in DCM and aggregate states.

and finally to 1.9-fold for **TPE-G3** as the f_a increased from 75% to 98%. This trend in the emission enhancement indicated that the TPE units in the core for higher-generation AIEgen-branched rotaxane dendrimers are less sensitive to the external environment changes attributed to the shielding effect.

In order to provide additional characterizations of the AIE behaviors of these rotaxane-branched dendrimers, we further investigated the aggregation of **TPE-G*n*** ($n = 1$, 2, and 3) through transmission electron microscopy (TEM) and dynamic light scattering (DLS) analysis. Based on previous DLS results, no aggregation of rotaxane-branched dendrimers was found in pure CH_2Cl_2 solution. However, when f_a was increased to 98%, the average D_h significantly increased to 80.5 nm (**TPE-G1**), 79.1 nm (**TPE-G2**), and 95.2 nm (**TPE-G3**), clearly indicating the formation of nanoscale aggregates (Fig. 3d–f). In addition, TEM images further showed that all AIEgen-branched rotaxane dendrimers formed homogenous spherical nanoparticles at fraction of 98% (for **TPE-G1**, 68.9 nm; for **TPE-G2**, 69.2 nm; for **TPE-G3**, 83.0 nm). It is worth noting that the size changes and trends of spherical particles obtained by TEM (Fig. S63†) were consistent with the average hydrodynamic diameter (D_h) values measured by DLS.

According to the above results, we have successfully synthesized a novel type of AIEgen-branched rotaxane dendrimers with up to a total of 42 AIEgens precisely distributed within the dendritic skeleton, which exhibited very interesting generation-dependent AIE performances. To further explore the potential applications of these new AIE-active macromolecules, we then explored their use for the construction of novel artificial LHSs. In the resulting LHSs, TPE units can serve as the fluorescence energy donors, so we chose eosin Y (ESY) as the fluorescence energy acceptor (Fig. 4a). Firstly, it was confirmed through DLS and TEM that an integrated aggregate of **TPE-G*n*** ($n = 1$, 2, and 3) and ESY was successfully formed. For example, when mixing ESY and **TPE-G*n*** ($n = 1$, 2, and 3) in aggregate state (ESY to TPE in a 1 : 3 ratio), DLS analysis suggested a slight increase in the average hydrodynamic diameter (D_h), and a similar trend was also observed from TEM analysis, suggesting the successful formation of integrated aggregates (Fig. S60–S63†).

Furthermore, by testing the emission spectra of rotaxane-branched dendrimers **TPE-G*n*** ($n = 1$, 2, and 3) and the adsorption spectrum of ESY, the possibility of effective energy transfer between **TPE-G*n*** ($n = 1$, 2, and 3) and ESY was verified. As shown in Fig. S38,† the two spectra overlapped very well, indicating that the artificial LHSs were feasible. To confirm this hypothesis, the emission spectra of **TPE-G*n*** ($n = 1$, 2, and 3) and ESY were studied by changing the ratios of ESY in the integrated system. As shown in Fig. 4b–d, when excited at a wavelength of 345 nm, the fluorescence emission intensity attributed to the energy donor TPE units at 480 nm gradually decreased. At the same time, a new fluorescence emission peak belonging to ESY appeared near 550 nm and increased with the increase of the acceptor upon excitation at 345 nm, demonstrating a typical energy transfer process. It is worth noting that as the energy acceptor ESY increased, there were slight hypochromic shifts in the emission wavelength of TPE and bathochromic shifts in the emission wavelength of ESY, indicating that there was a certain intermolecular interaction between the rotaxane-branched dendrimers and ESY in the aggregated state of the artificial

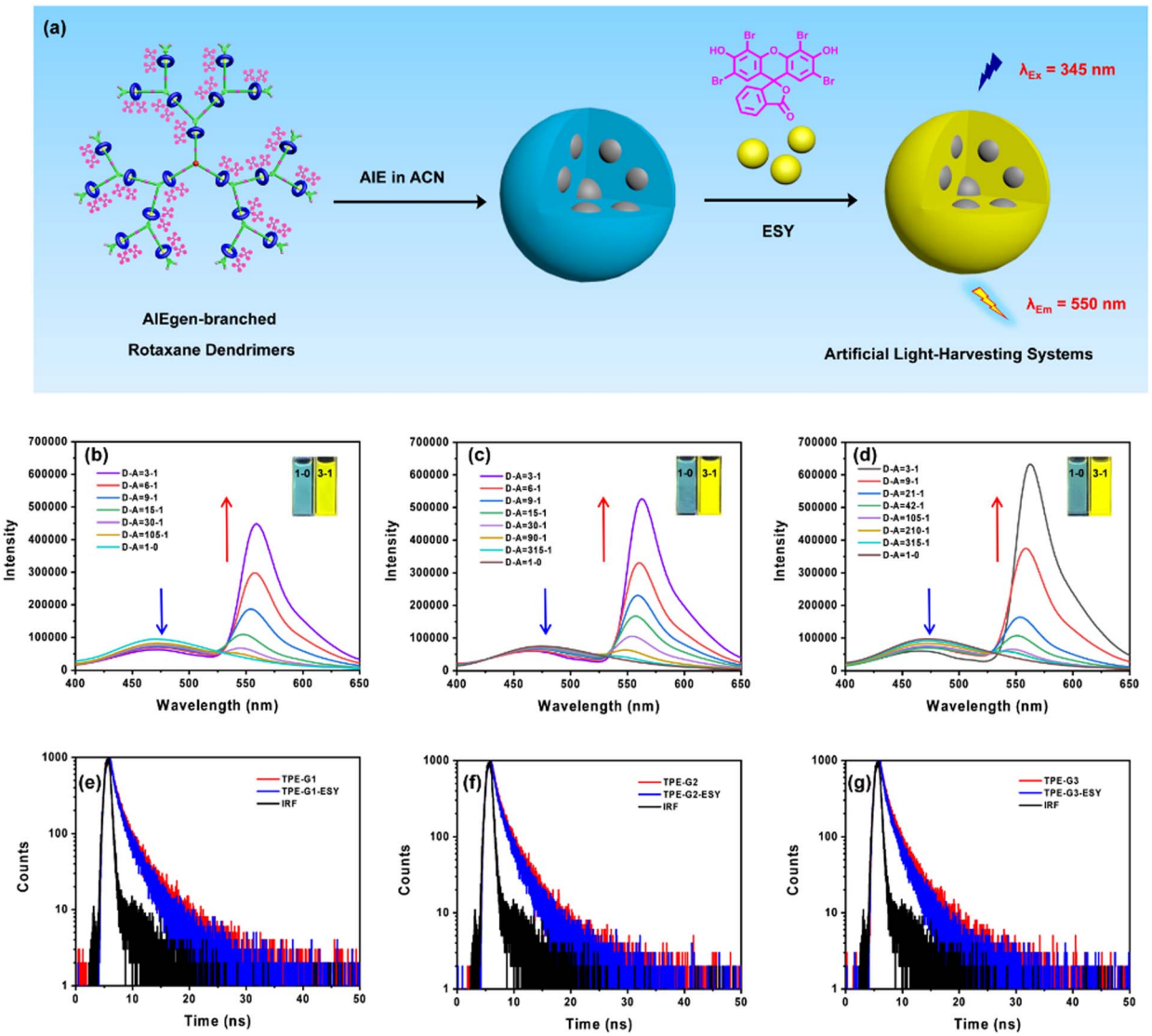

Fig. 4 (a) The construction of artificial LHSs based on AIEgen-branched rotaxane dendrimers **TPE-G*n*** (donor, $n = 1$, 2, and 3) and ESY (acceptor). Representation of LHSs based on the AIEgen-branched rotaxane dendrimer **TPE-G3** and ESY. Fluorescence spectra of **TPE-G1** (b), **TPE-G2** (c), and **TPE-G3** (d) with different ratios of ESY in **TPE-G*n*-ESY** ([TPE units] = 50 μM, $\lambda_{ex} = 345$ nm); inset: photograph of **TPE-G*n*-ESY** in DCM/ACN with 98% ACN fractions upon UV excitation ($\lambda_{ex} = 365$ nm); Time-resolved fluorescence decay curves for **TPE-G1** and **TPE-G1-ESY** (e), **TPE-G2** and **TPE-G2-ESY** (f), **TPE-G3** and **TPE-G3-ESY** (g) in the aggregate state (375 nm excitation and 480 nm detection).

LHSs. According to the above experimental results, it can be further demonstrated that the artificial LHSs based on novel AIEgen-branched rotaxane dendrimers have been successfully constructed, which could undergo efficient energy transfer process. In addition, based on the ratios of the fluorescence emission intensities of TPE units in rotaxane-branched dendrimers, the energy transfer efficiencies (Φ_{ET}) were calculated to be 34.5% (**TPE-G1-ESY**), 31.9% (**TPE-G2-ESY**), and 39.4% (**TPE-G3-ESY**), respectively (Figures S42–S44†). Moreover, the antenna effects (AE) were measured to be 1.09 (**TPE-G1-ESY**), 1.11 (**TPE-G2-ESY**), and 1.79 (**TPE-G3-ESY**), respectively (Fig. S45–S47†). To further confirm the effective energy transfer process of the resultant artificial LHSs, the fluorescence lifetimes (τ) of the relevant energy donors and acceptors obtained by doping ESY into the rotaxane-branched dendrimers were characterized using time-correlated single-photon counting (TCSPC) tests. The fluorescence decay curves of **TPE-G*n*** ($n = 1$, 2, and 3) and the artificial LHSs **TPE-G*n*-ESY** ($n = 1$, 2, and 3) were monitored at the wavelength of 480 nm, and attributed to the energy donor upon excitation at 375 nm. As shown in Fig. 4e–g, when the molar ratio of the TPE units to ESY was 3 : 1, the fluorescence lifetimes of the TPE units in the rotaxane-branched dendrimers **TPE-G*n*** ($n = 1$, 2, and 3) was obtained through mono exponential decay function fitting: $\tau = 2.56$ ns (**TPE-G1**), $\tau = 2.24$ ns (**TPE-G2**), and $\tau = 2.28$ ns (**TPE-G3**). However, in the corresponding artificial LHSs **TPE-G*n*-ESY** ($n = 1$, 2, and 3), the fluorescence lifetimes of the TPE units decreased to $\tau = 2.27$ ns (**TPE-G1-ESY**), $\tau = 2.06$ ns (**TPE-G2-ESY**), and $\tau = 2.03$ ns (**TPE-**

G3-ESY), clearly demonstrating the effective energy transfer process between the TPE units and ESY.

Furthermore, due to the presence of the urea moiety, we studied the emission spectra of the AIEgen-branched rotaxane dendrimers and the corresponding artificial LHSs under external stimuli. Notably, upon the addition of trifluoroacetate anions, we observed a remarkable enhancement in the emission spectra of **TPE-G*n*** (n = 1, 2, and 3), accompanied by an enhancement in the energy transfer efficiency of the artificial LHSs (Fig. S52–S54†). These results demonstrated that the anion-induced stimuli responsiveness can efficiently boost both the AIE properties of the AIEgen-branched rotaxane dendrimers and the energy transfer efficiency of artificial LHSs through induction of the wheel movements, thereby highlighting the crucial role of mechanical bonds in developing novel stimuli-responsive artificial LHSs.

Photocatalyzed functionalization of C–H bonds by artificial light harvesting systems

To further mimic the important light harvesting process of converting light energy into chemical energy in natural photosynthesis, we further investigated the application of the resulting artificial light harvesting systems based on rotaxane-branched dendrimers. Since ESY is a widely used photosensitive catalyst,[21] the novel artificial LHSs are expected to be excellent catalysts for photocatalytic reactions. To evaluate the catalytic performances of the LHSs, we chose the C–H bond alkylation reaction through free radical addition to dicyanide electron-deficient olefin as the model reaction (Table 1). To our delight, for the reaction of 2-benzylidenepropanedinitrile (**1a**) and benzaldehyde (**2a**), the employment of only 1.0 mol% LHS **TPE-G1-ESY** as the catalyst resulted in both high efficiency and high yield (nearly 90%) (entry 10). By comparison, eosin Y alone could not catalyze the reaction, and only trace amounts of product were detected (entry 2). In addition to ESY, RB and RhB were employed for the construction of artificial LHSs for photocatalysis. However, as summarized in Table 1, the corresponding artificial LHSs **TPE-G1-RB** and **TPE-R1-RhB** revealed relatively poorer catalytic performances, possibly attributed to the low energy transfer efficiency and antenna effect. In addition, in the absence of ESY, **TPE-R** and **TPE-G1** were also noneffective (entries 5 and 6). When **TPE-G1-ESY** was employed as the photocatalyst, the complete conversion was achieved within 12 hours (entry 10). In stark contrast, owing to the weak emission of **TPE-R**, the **TPE-R-ESY** system exhibited significantly reduced catalytic performance (entry 9). Even after a prolonged reaction time of 24 hours, **TPE-R-ESY** system only led to a poor yield of 12%, which indicated that the integrated artificial LHSs based on AIEgen-branched rotaxane dendrimer indeed significantly enhanced the photocatalytic performances. In addition, we further investigated the photocatalytic performances of artificial LHS **TPE-G1-ESY** under stimuli responsiveness. The results revealed that the introduction of trifluoroacetate anions led to an enhanced reaction rate with decreased reaction time to 10 hours, while maintaining a high yield of 89% (entry 12). In contrast, when the artificial LHS **TPE-G1-ESY** was tested without the stimulus under the same reaction time of 10 hours, the yield reached only 78% (entry 11). These findings further highlight that the introduction of urea-responsive sites in these mechanically bonded dendrimers provides a new method for modulating the photocatalytic efficiency of corresponding artificial LHSs.

Table 1 Catalyst comparison data for the functionalization of inert C–H bonds

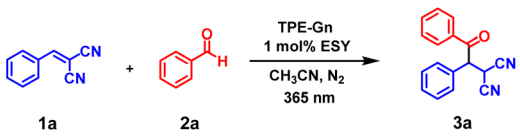

1a 2a 3a

Entry	Catalyst	Time	Yield[a] (%)
1	No cat.	24 h	None
2	ESY	24 h	Trace
3	RB	24 h	Trace
4	RhB	24 h	Trace
5	**TPE-R**	24 h	Trace
6	**TPE-G1**	24 h	Trace
7	**TPE-G1-RB**	24 h	15%
8	**TPE-G1-RhB**	24 h	56%
9	**TPE-R-ESY**	24 h	12%
10	**TPE-G1-ESY**	12 h	90%
11	**TPE-G1-ESY**	10 h	78%
12	**TPE-G1-ESY** + CF_3COO^-	10 h	89%
13	**TPE-G2-ESY**	4 h	96%
14	**TPE-G3-ESY**	2.5 h	92%

[a] Isolated yields of products after column chromatography.

Notably, when **TPE-G2-ESY** or **TPE-G3-ESY** was employed as the photocatalyst, the time was further reduced to 4.0 hours and 2.5 hours with enhanced isolated yields of 96% and 92% (entry 13 and 14), respectively, suggesting an interesting generation effect of the rotaxane-branched dendrimers on the photocatalytic performances, particularly the reaction rates of the corresponding LHSs. Such effect might be attributed to the following factors: with the increase of the dendrimer generation, the higher donor/acceptor ratio enhances the light absorption by more TPE units; the greater structural rigidity and more densely-packed architecture leads to more efficient energy transfer and electron–hole separation; and the larger size and branched architecture provides a more accessible environment for substrate interaction with the catalytic sites.

Due to the high catalytic activity of these novel LHSs, we further used **TPE-G1-ESY** as the photocatalyst to investigate the scope of the coupling reactions. As shown in Scheme 1, the desired catalytic products could be obtained in satisfactory yields (up to 99%) for various substrates **2a** with either electron-withdrawing groups or the electron-donating groups (**3b** to **3g**), and the position of the substituents had little influence on the yields of the reactions (**3b** to **3d**). In addition, a substrate with a larger steric hindrance was applicable for this reaction (**3j**). It is worth mentioning that the modification of the substrate **1a** could also produce corresponding products with good to

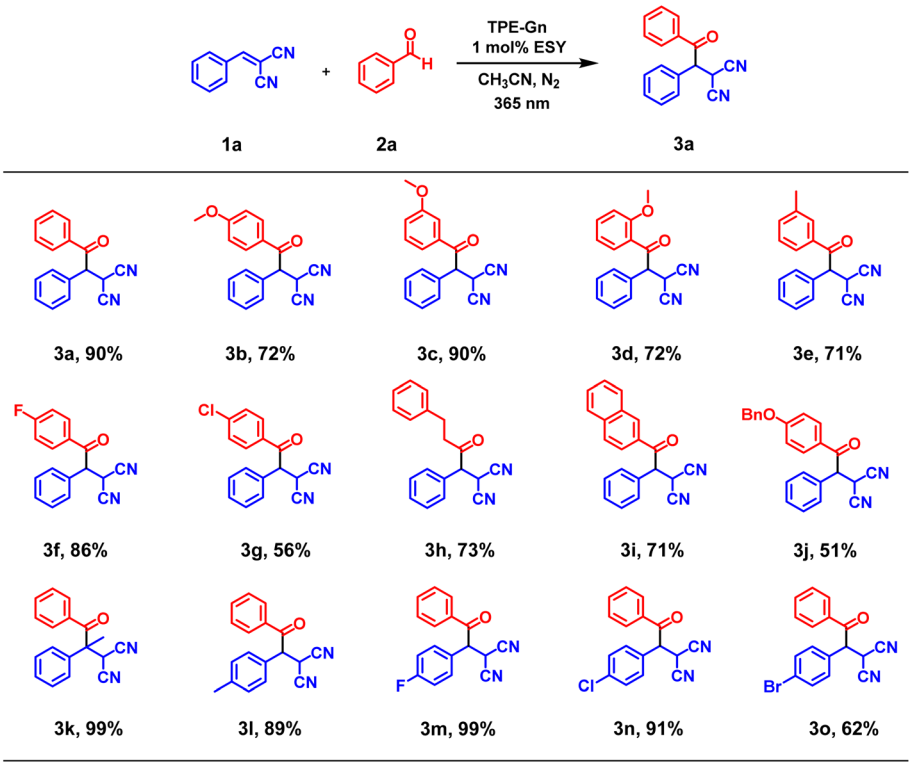

Scheme 1 Scope of the artificial LHS **TPE-G1-ESY**-catalyzed functionalization of inert C–H bonds.

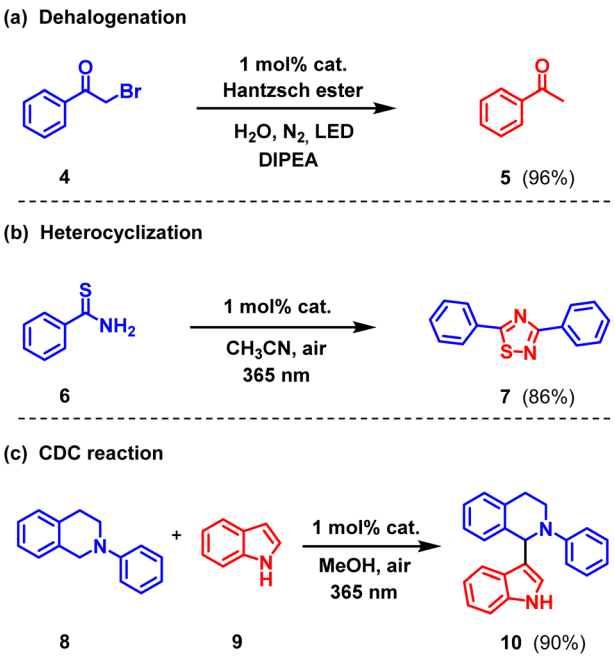

Scheme 2 Extended photocatalytic reaction types catalyzed by artificial LHS **TPE-G1-ESY**.

excellent yields (**3k** to **3o**), indicating that artificial LHSs constructed from AIEgen-branched rotaxane dendrimers can serve as effective photocatalysts for various chemical transformations. Notably, compared with previous reports, the employment of artificial LHSs as photocatalysts revealed some attractive advantages, such as lower catalyst loading, higher reaction rates, and wider substrate scope, highlighting the key role of the formation of artificial LHSs in the enhancement of photocatalytic performances. The possible mechanism of this photocatalyzed reaction is shown in Scheme S6:† the LHSs **TPE-G*n*-ESY** as the photosensitizer (PS) were irradiated by UV illumination ($\lambda_{ex} = 365$ nm) to form a high-energy excited state PS*, which captured a hydrogen atom from the substrate through HAT, generating a carbon-centric radical, thereby activating the substrate. Subsequently, the carbon-centric radical was captured by electron-deficient olefin to form a radical intermediate. The intermediate and PS-H ultimately produced coupling products through the RHAT process, simultaneously achieving the regeneration of PS.

To evaluate the reaction scope of the artificial LHSs as photocatalysts, additional dehalogenation, heterocyclization, and aerobic cross-dehydrogenative coupling (CDC) reactions were further tested in addition to the photocatalyzed functionalization of C–H bonds. To our delight, as shown in Scheme 2 and Tables S3–S5,† the artificial LHSs based on the newly-developed AIEgen-branched rotaxane dendrimers exhibited excellent catalytic performances across all of these reaction types, highlighting the great potential of AIEgen-branched rotaxane dendrimers for application in photocatalysis.

Conclusions

In conclusion, we have successfully realized the construction of a novel type of AIEgen-branched rotaxane dendrimers with up

to 42 TPE units precisely distributed within the dendrimer skeletons. Based on such high-density topological arrangements of AIEgens, the free movements of the AIEgen units with the dendrimer skeletons exhibited a more significant steric hindrance effect, thereby not only enhancing the AIE effect but also improving the AIE performances. By selecting ESY as the energy acceptor, novel artificial LHSs based on these AIEgen-branched rotaxane dendrimers have been successfully constructed through the efficient FRET process, which proved to be excellent photocatalysts for the activation of inert C–H bonds through a typical HAT process to enable their functionalization. Interestingly, LHSs based on higher generation AIEgen-branched rotaxane dendrimers exhibited significantly enhanced catalytic performances, indicating a remarkable generation effect. This study successfully realized the synthesis of a novel type of high-density AIEgen-branched rotaxane dendrimers for the first time, providing a promising platform for the construction of smart luminescent materials for practical use. In particular, considering the unique planar chirality of the pillar[5]arene wheel with the AIEgen-branched rotaxane dendrimers, the corresponding artificial LHSs based on chiral dendrimers would show great potential for applications in asymmetric photocatalysis.

Data availability

The data supporting this article have been included as part of the ESI.†

Author contributions

Conceptualization, X.-Q. X., X.-Q. W., H.-B. Y., W. W.; methodology, X.-Q. X., Y.-R. S., J.-H.C.; investigation, X.-Q. X., W.-J. L., Y. Z., D.-Y. Z.; data curation, X.-Q. X., J.-H.C., W.-J. L.; writing, X.-Q. X., X.-Q. W., H.-B. Y., W. W.; supervision, X.-Q. W., H.-B. Y.; project administration, X.-Q. X.; funding acquisition, H.-B. Y., X.-Q. W., W. W.

Conflicts of interest

There are no conflicts to declare.

Acknowledgements

H.-B. Y. acknowledges the financial support sponsored by the National Key R&D Program of China (2021YFA1501600). X.-Q. W. acknowledges the financial support sponsored by the National Natural Science Foundation of China (22201077). W. W. acknowledges the financial support sponsored by the Natural Science Foundation of Shanghai (23ZR1419600).

Notes and references

1 (*a*) R. Croce and H. van Amerongen, *Nat. Chem. Biol.*, 2014, **10**, 492–501; (*b*) G. D. Scholes, G. R. Fleming, A. Olaya-Castro and R. van Grondelle, *Nat. Chem.*, 2011, **3**, 763–774; (*c*) P. D. Frischmann and K. Mahata, *Chem. Soc. Rev.*, 2013, **42**, 1847–1870; (*d*) T. Mirkovic, E. E. Ostroumov, J. M. Anna, R. van Grondelle, Govindjee and G. D. Scholes, *Chem. Rev.*, 2017, **117**, 249–293.

2 G. McDermott, S. M. Prince, A. A. Freer, A. M. Hawthornthwaite-Lawless, M. Z. Papiz, R. J. Cogdell and N. W. Isaacs, *Nature*, 1995, **374**, 517–521.

3 (*a*) M. Zhang, S. Yin, J. Zhang, Z. Zhou, M. L. Saha, C. Lu and P. J. Stang, *Proc. Natl. Acad. Sci. U.S.A.*, 2017, **114**, 3044–3049; (*b*) R. J. Sension, *Nature*, 2007, **446**, 740–741; (*c*) X. Qin, M. Suga, T. Kuang and J.-R. Shen, *Science*, 2015, **348**, 989–995; (*d*) J. Lv, J. Xie, A. G. A. Mohamed, X. Zhang, Y. Feng, L. Jiao, E. Zhou, D. Yuan and Y. Wang, *Nat. Rev. Chem*, 2023, **7**, 91–105; (*e*) R. Croce and H. van Amerongen, *Science*, 2020, **369**, 2058.

4 (*a*) N. Aratani, D. Kim and A. Osuka, *Acc. Chem. Res.*, 2009, **42**, 1922–1934; (*b*) Y. Nakamura, N. Aratani and A. Osuka, *Chem. Soc. Rev.*, 2007, **36**, 831–845; (*c*) J. Yang, M.-C. Yoon, H. Yoo, P. Kim and D. Kim, *Chem. Soc. Rev.*, 2012, **41**, 4808–4826; (*d*) D. Yim, J. Sung, S. Kim, J. Oh, H. Yoon, Y. M. Sung, D. Kim and D. Yang, *J. Am. Chem. Soc.*, 2017, **139**, 993–1002; (*e*) G. B. Bodedla, M. Imran, J. Zhao, X. Zhu and W.-Y. Wong, *Aggregate*, 2023, **4**, e364; (*f*) M.-S. Choi, T. Yamazaki, I. Yamazaki and T. Aida, *Angew. Chem., Int. Ed.*, 2004, **43**, 150–158; (*g*) Y. Liu, *Angew. Chem., Int. Ed.*, 2016, **55**, 7952–7957; (*h*) A. Uetomo, *J. Am. Chem. Soc.*, 2011, **133**, 13276–13279.

5 (*a*) Q. Zou, K. Liu, M. Abbas and X. Yan, *Adv. Mater.*, 2016, **28**, 1031–1043; (*b*) Y.-H. Jeong, M. Son, H. Yoon, P. Kim, D.-H. Lee, D. Kim and W.-D. Jang, *Angew. Chem., Int. Ed.*, 2014, **53**, 6925–6928; (*c*) W.-Q. Wu, H.-L. Feng, H.-S. Rao, Y.-F. Xu, D.-B. Kuang and C.-Y. Su, *Nat. Commun.*, 2014, **5**, 3968; (*d*) C. Devadoss, P. Bharathi and J. S. Moore, *J. Am. Chem. Soc.*, 1996, **118**, 9635–9644; (*e*) W. R. Dichtel, S. Hecht and J. M. J. Fréchet, *Org. Lett.*, 2005, **7**, 4451–4454; (*f*) X.-H. Jeong, *Angew. Chem., Int. Ed.*, 2014, **53**, 6925–6928; (*g*) Y. Zeng, Y. Li, M. Li, G. Yang and Y. Li, *J. Am. Chem. Soc.*, 2009, **131**, 9100–9106.

6 (*a*) K. V. Rao, K. K. R. Datta, M. Eswaramoorthy and S. J. George, *Angew. Chem., Int. Ed.*, 2011, **50**, 1179–1184; (*b*) R. Sethy, J. Kumar, R. Métivier, M. Louis, K. Nakatani, N. M. T. Mecheri, A. Subhakumari, K. G. Thomas, T. Kawai and T. Nakashima, *Angew. Chem., Int. Ed.*, 2017, **56**, 15053–15057; (*c*) X. Li, Y. Wang, A. Song, M. Zhang, M. Chen, M. Jiang, S. Yu, R. Wang and L. Xin, *Chin. J. Chem.*, 2021, **39**, 2725–2730.

7 (*a*) D. E. Williams, J. A. Rietman, J. M. Maier, R. Tan, A. B. Greytak, M. D. Smith, J. A. Krause and N. B. Shustova, *J. Am. Chem. Soc.*, 2014, **136**, 11886–11889; (*b*) J. Yu, R. Anderson, X. Li, W. Xu, S. Goswami, S. S. Rajasree, K. Maindan, D. A. Gómez-Gualdrón and P. Deria, *J. Am. Chem. Soc.*, 2020, **142**, 11192–11202; (*c*) M. C. So, G. P. Wiederrecht, J. E. Mondloch, J. T. Hupp and O. K. Farha, *Chem. Commun.*, 2015, **51**, 3501–3510; (*d*) S. Chen, K. Li, F. Zhao, L. Zhang, M. Pan, Y.-Z. Fan, J. Guo, J. Shi and C.-Y. Su, *Nat. Commun.*, 2016, **7**, 13169; (*e*) X. Li,

J. Yu, D. J. Gosztola, H. C. Fry and P. Deria, *J. Am. Chem. Soc.*, 2019, **141**, 16849.

8 (*a*) Y. Jiang and J. McNeill, *Chem. Rev.*, 2017, **117**, 838–859; (*b*) H. Qian, T. Xiao and R. B. P. Elmes, *Chin. Chem. Lett.*, 2023, **34**, 108185; (*c*) L. Xu, Z. Wang, R. Wang, L. Wang, X. He, H. Jiang, H. Tang, D. Cao and B. Z. Tang, *Angew. Chem., Int. Ed.*, 2020, **59**, 9908–9913; (*d*) Y. Shi, X. Cao, D. Hu and H. Gao, *Angew. Chem., Int. Ed.*, 2018, **57**, 516–520; (*e*) J. Zhang, C. Yang, R. Zhang, R. Chen, Z. Zhang, W. Zhang, S.-H. Peng, X. Chen, G. Liu, C.-S. Hsu and C.-S. Lee, *Adv. Funct. Mater.*, 2017, **27**, 1605094; (*f*) S. Hirayama, K. Oohora, T. Uchihashi and T. Hayashi, *J. Am. Chem. Soc.*, 2020, **142**, 1822–1831; (*g*) B. Song, L. Zhang, J. Sun, J. W. Y. Lam and B. Z. Tang, *Angew. Chem., Int. Ed.*, 2023, **62**, e202302543.

9 P.-Z. Chen, Y.-X. Weng, L.-Y. Niu, Y.-Z. Chen, L.-Z. Wu, C.-H. Tung and Q.-Z. Yang, *Angew. Chem., Int. Ed.*, 2016, **55**, 2759–2763.

10 (*a*) Z. Xu, S. Peng, Y.-Y. Wang, J.-K. Zhang, A. I. Lazar and D.-S. Guo, *Adv. Mater.*, 2016, **28**, 7666–7671; (*b*) B. Mu, X. Hao, X. Luo, Z. Yang, H. Lu and W. Tian, *Nat. Commun.*, 2024, **15**, 903; (*c*) D. Bokotial, Ko. Acharyya, A. Chowdhury and P. S. Mukherjee, *Angew. Chem., Int. Ed.*, 2024, **63**, e202401136; (*d*) L. Shao, D. Hu, S.-Li. Zheng, T. K. H. Trinh, W. Zhou, H. Wang, Y. Zong, C. Li and C.-L. Chen, *Angew. Chem., Int. Ed.*, 2024, **63**, e202403263; (*e*) Y. Wu, Y. Wang, X. Yu and Q. Song, *Adv. Sci.*, 2024, **11**, e2404269; (*f*) Y. Han, X. Zhang, Z. Ge, Z. Gao, R. Liao and F. Wang, *Nat. Commun.*, 2022, **13**, 3546; (*g*) L. Tu, Y. Chen, X. Song, W. Jiang, Y. Xie and Z. Li, *Angew. Chem., Int. Ed.*, 2024, **63**, e202402865; (*h*) Q. Zhang, X. Dang, F. Cui and T. Xiao, *Chem. Commun.*, 2024, **60**, 10064; (*i*) S. Yu, R.-X. Zhu, K.-K. Niu, N. Han, H. Liu and L.-B. Xing, *Chem. Sci.*, 2024, **15**, 1870; (*j*) Z. Lian, J. He, L. Liu, Y. Fan, X. Chen and H. Jiang, *Nat. Commun.*, 2023, **14**, 2752; (*k*) Y.-X. Yuan, J.-N. Zhang, J.-R. Wang, K. Li and S.-Q. Zang, *Chem*, 2024, **10**, 1766–1782; (*l*) R.-Z. Zhang, K.-K. Niu, Y.-S. Bi, H. Liu, N. Han and L.-B. Xing, *Small*, 2024, 2405564; (*m*) G.-L. Li, K.-K. Niu, X.-Z. Yang, H. Liu, S. Yu and L.-B. Xing, *J. Mater. Chem. A*, 2024, **12**, 13356; (*n*) H. Li, J. Yang, D. Li, X. Li, J. Li and C. He, *Angew. Chem., Int. Ed.*, 2024, **63**, e202409094; (*o*) X. Zhou, X. Bai, F. Shang, H.-Y. Zhang, L.-H. Wang, X. Xu and Y. Liu, *Nat. Commun.*, 2024, **15**, 4787; (*p*) R. Feng, X. Yan, Y. Sang, X. Liu, Z. Luo, Z. Xie, Y. Ke and Q. Song, *Angew. Chem., Int. Ed.*, 2024, e202421729; (*q*) K. Yang, R. Zhang, Y. Liu, B. Zhao, Y. Wu and J. Deng, *Angew. Chem., Int. Ed.*, 2024, **63**, e202409514; (*r*) T. Li, D. Niu, L. Ji, Q. Li, B. Guan, H. Wang, G. Ouyang and M. Liu, *Nat. Commun.*, 2025, **16**, 1698; (*s*) S. Yu, R.-X. Zhu, K.-K. Niu, N. Han and L.-B. Xing, *Chem. Sci.*, 2024, **15**, 1870–1878; (*t*) M. Yang, Y. Sun, X. Wang, J. Wang, Y. Liu, A. Zhang, J. Shen and W. Qi, *Adv. Opt. Mater.*, 2025, 2403539; (*u*) J.-C. Yang, K. Chen, G.-L. Zhang, C. Qi, H.-T. Feng and B. Z. Tang, *Chem. Sci.*, 2025, DOI: 10.1039/d4sc07689c.

11 (*a*) H.-Q. Peng, L.-Y. Niu, Y.-Z. Chen, L.-Z. Wu, C.-H. Tung and Q.-Z. Yang, *Chem. Rev.*, 2015, **115**, 7502–7542; (*b*) K. Acharyya, S. Bhattacharyya, S. Lu, Y. Sun, P. S. Mukherjee and P. J. Stang, *Angew. Chem., Int. Ed.*, 2022, **61**, e202200715; (*c*) Y.-X. Hu, W.-J. Li, P.-P. Jia, X.-Q. Wang, L. Xu and H.-B. Yang, *Adv. Opt. Mater.*, 2020, **8**, 2000265; (*d*) Z. Zhang, Z. Zhao, Y. Hou, H. Wang, X. Li, G. He and M. Zhang, *Angew. Chem., Int. Ed.*, 2019, **58**, 8862–8866; (*e*) D. Zhang, W. Yu, S. Li, Y. Xia, X. Li, Y. Li and T. Yi, *J. Am. Chem. Soc.*, 2021, **143**, 1313–1317; (*f*) Z. Zhang, Z. Zhao, L. Wu, S. Lu, S. Ling, G. Li, L. Xu, L. Ma, Y. Hou, X. Wang, X. Li, G. He, K. Wang, B. Zou and M. Zhang, *J. Am. Chem. Soc.*, 2020, **142**, 2592–2600; (*g*) Y. Qin, Q.-H. Ling, Y.-T. Wang, Y.-X. Hu, L. Hu, X. Zhao, D. Wang, H.-B. Yang, L. Xu and B. Z. Tang, *Angew. Chem., Int. Ed.*, 2023, **62**, e202308210; (*h*) D. Li, L. Yang, W. Fang, X. Fu, H. Li, J. Li and X. Li, *Chem. Sci.*, 2023, **14**, 9943–9950; (*i*) C.-B. Huang, L. Xu, J.-L. Zhu, Y.-X. Wang, B. Sun, X. Li and H.-B. Yang, *J. Am. Chem. Soc.*, 2017, **139**, 9459–9462; (*j*) H.-Q. Peng, Y.-Z. Chen, Y. Zhao, Q.-Z. Yang, L.-Z. Wu, C.-H. Tung, L.-P. Zhang and Q. X. Tong, *Angew. Chem., Int. Ed.*, 2012, **51**, 2088–2092; (*k*) M. Chen, Z. Lu, M. Li, B. Jiang, S. Liu, Y. Li, B. Zhang, X. Li, T. Yi and D. Zhang, *Adv. Healthcare Mater.*, 2023, **12**, 2300377; (*l*) Q. Liu, M. Zuo, K. Wang and X.-Y. Hu, *Chem. Commun.*, 2023, **59**, 13707–13710; (*m*) K. Wang, Y. Shen, P. Jeyakkumar, Y. Zhang, L. Chu, R. Zhang and X.-Y. Hu, *Curr. Opin. Green Sustainable Chem.*, 2023, **41**, 100823.

12 (*a*) X.-M. Chen, Q. Cao, H. K. Bisoyi, M. Wang, H. Yang and Q. Li, *Angew. Chem., Int. Ed.*, 2020, **59**, 10493–10497; (*b*) Y.-X. Yuan, J.-H. Jia, Y.-P. Song, F.-Y. Ye, Y.-S. Zheng and S.-Q. Zang, *J. Am. Chem. Soc.*, 2022, **144**, 5389–5399; (*c*) H. Chen, W. Liu, A. Laemont, C. Krishnaraj, X. Feng, F. Rohman, M. Meledina, Q. Zhang, R. V. Deun, K. Leus and P. V. D. Voort, *Angew. Chem., Int. Ed.*, 2021, **60**, 10820–10827; (*d*) M. Hao, G. Sun, M. Zuo, Z. Xu, Y. Chen, X.-Y. Hu and L. Wang, *Angew. Chem., Int. Ed.*, 2020, **59**, 10095–10100; (*e*) D. Zhang, M. Li, B. Jiang, S. Liu, J. Yang, X. Yang, K. Ma, X. Yuan and T. Yi, *J. Colloid Interface Sci.*, 2023, **652**, 1494–1502; (*f*) S. Guo, Y. Song, Y. He, X.-Y. Hu and L. Wang, *Angew. Chem., Int. Ed.*, 2018, **57**, 3163–3167; (*g*) Y. Li, S. S. Rajasree, G. Y. Lee, J. Yu, J.-H. Tang, R. Ni, G. Li, K. N. Houk, P. Deria and P. J. Stang, *J. Am. Chem. Soc.*, 2021, **143**, 2908–2919; (*h*) Z. Wu, H. Qian, X. Li, T. Xiao and L. Wang, *Chin. Chem. Lett.*, 2024, **35**, 108829; (*i*) X. Tang, Y. Zhu, W. Guan and C. Lu, *Aggregate*, 2023, **4**, e348; (*j*) H. Shang, X. Le, Y. Sun, S. Wu, Y. Wang, P. Théato and T. Chen, *Mater. Horiz.*, 2024, **11**, 2856.

13 (*a*) Y. Zeng, Y. Li, M. Li, G. Yang and Y. Li, *J. Am. Chem. Soc.*, 2009, **131**, 9100–9106; (*b*) F. C. De Schryver, T. Vosch, M. Cotlet, M. Van der Auweraer, K. Müllen and J. Hofkens, *Acc. Chem. Res.*, 2005, **38**, 514–522.

14 J. Luo, Z. Xie, J. W. Y. Lam, L. Cheng, H. Chen, C. Qiu, H. S. Kwok, X. Zhan, Y. Liu, D. Zhu and B. Z. Tang, *Chem. Commun.*, 2001, **18**, 1740–1741.

15 (*a*) J. Hwang, P. Nagaraju, M. J. Cho and D. H. Choi, *Aggregate*, 2023, **4**, e199; (*b*) C. Mu, L. Zhang, G. Li, Y. Hou, H. Liu, Z. Zhang, R. Zhang, T. Gao, Y. Qian, C. Guo, G. He and M. Zhang, *Angew. Chem., Int. Ed.*, 2023, **62**,

e202311137; (*c*) H. Yan, X. Yin, D. Wang, T. Han and B. Z. Tang, *Adv. Sci.*, 2023, **10**, 2305149; (*d*) H. Liu, Z. Zhang, C. Mu, L. Ma, H. Yuan, S. Ling, H. Wang, X. Li and M. Zhang, *Angew. Chem., Int. Ed.*, 2022, **61**, e202207289; (*e*) H. Yan, Y. He, D. Wang, T. Han and B. Z. Tang, *Aggregate*, 2023, **4**, e331; (*f*) Y. Sun, K. Wang, X. Huang, S. Wei, E. Contreras, P. K. Jain, L. M. Campos, H. J. Kulik and J. S. Moore, *J. Am. Chem. Soc.*, 2024, **146**, 27117–27126; (*g*) Z. Guo, G. Li, H. Wang, J. Zhao, Y. Liu, H. Tan, X. Li, P. J. Stang and X. Yan, *J. Am. Chem. Soc.*, 2021, **143**, 9215–9221.

16 (*a*) W.-S. Li and T. Aida, *Chem. Rev.*, 2009, **109**, 6047–6076; (*b*) D. Astruc, E. Boisselier and C. Ornelas, *Chem. Rev.*, 2010, **110**, 1857–1959; (*c*) F. Vögtle, G. Richardt and N. Werber, *Dendrimer Chemistry: Concepts, Syntheses, Properties, Applications*, Wiley-VCH, Weinheim, 2009; (*d*) V. Balzani, S. Campagna, G. Denti, A. Juris, S. Serroni and M. Venturi, *Acc. Chem. Res.*, 1998, **31**, 26–34.

17 (*a*) B. Xu, J. Zhang, H. Fang, S. Ma, Q. Chen, H. Sun, C. Im and W. Tian, *Polym. Chem.*, 2014, **5**, 479–488; (*b*) X.-Q. Wang, W. Wang, W.-J. Li, Y. Qin, G.-Q. Yin, W.-L. Jiang, X. Li, S. Wu and H.-B. Yang, *Org. Chem. Front.*, 2019, **6**, 1686–1691; (*c*) M. Arseneault, N. L. C. Leung, L. T. Fung, R. Hu, J.-F. Morin and B. Z. Tang, *Polym. Chem.*, 2014, **5**, 6087–6096.

18 W.-J. Li, X.-Q. Wang, D.-Y. Zhang, Y.-X. Hu, W.-T. Xu, L. Xu, W. Wang and H.-B. Yang, *Angew. Chem., Int. Ed.*, 2021, **60**, 18761–18768.

19 (*a*) G.-Y. Wu, X. Shi, H. Phan, H. Qu, Y.-X. Hu, G.-Q. Yin, X.-L. Zhao, X. Li, L. Xu, Q. Yu and H.-B. Yang, *Nat. Commun.*, 2020, **11**, 3178; (*b*) Y. Wang, S. Lu, X.-Q. Wang, Y.-F. Niu, H. Wang and W. Wang, *Org. Chem. Front.*, 2021, **8**, 4994–5001; (*c*) Y. Wang, J. Gong, X. Wang, W.-J. Li, X.-Q. Wang, X. He, W. Wang and H.-B. Yang, *Angew. Chem., Int. Ed.*, 2022, **61**, e202210542; (*d*) X.-Q. Xu, X.-Q. Wang and W. Wang, *Chin. Chem. Lett.*, 2023, **34**, 107665; (*e*) D.-Y. Zhang, Y. Sang, T. K. Das, Z. Guan, N. Zhong, C.-G. Duan, W. Wang, J. Fransson, R. Naaman and H.-B. Yang, *J. Am. Chem. Soc.*, 2023, **145**, 26791–26798; (*f*) D.-Y. Zhang, Y. Zheng, Y. Jiang, W.-J. Li, X.-Q. Wang, L. Hu, W. Wang and H.-B. Yang, *CCS Chem.*, 2024, **6**, 2162–2174; (*g*) Y. Wang, X. Zhang, C.-B. Huang, L. Hu, X.-Q. Wang, W. Wang and H.-B. Yang, *Angew. Chem., Int. Ed.*, 2024, **63**, e202408271; (*h*) Y. Wang, W.-L. Zhao, Z. Gao, C. Qu, X. Li, Y. Jiang, L. Hu, X.-Q. Wang, M. Li, W. Wang, C.-F. Chen and H.-B. Yang, *Angew. Chem., Int. Ed.*, 2025, **64**, e202417458; (*i*) W.-T. Xu, X. Li, P. Wu, W.-J. Li, Y. Wang, X.-Q. Xu, X.-Q. Wang, J. Chen, H.-B. Yang and W. Wang, *Angew. Chem., Int. Ed.*, 2024, **63**, e202319502; (*j*) Z. Peng, P.-P. Jia, X.-Q. Wang, X.-L. Zhao, H.-B. Yang and W. Wang, *CCS Chem.*, 2024, **6**, 2489–2501; (*k*) W.-J. Li, Q. Gu, X.-Q. Wang, D.-Y. Zhang, Y.-T. Wang, X. He, W. Wang and H.-B. Yang, *Angew. Chem., Int. Ed.*, 2021, **60**, 9507–9515; (*l*) X. Li, W.-T. Xu, X.-Q. Xu, Y. Wang, X.-Q. Wang, H.-B. Yang and W. Wang, *Angew. Chem., Int. Ed.*, 2025, **64**, e202412548; (*m*) J.-L. Song, C. Chen, X. Li, Y. Jiang, Z. Peng, X.-Q. Wang, H.-B. Yang and W. Wang, *Nat. Commun.*, 2024, **15**, 10531.

20 (*a*) W. Wang, L.-J. Chen, X.-Q. Wang, B. Sun, X. Li, Y. Zhang, J. Shi, Y. Yu, L. Zhang, M. Liu and H.-B. Yang, *Proc. Natl. Acad. Sci. U. S. A.*, 2015, **112**, 5597–5601; (*b*) X.-Q. Wang, W. Wang, W.-J. Li, L.-J. Chen, R. Yao, G.-Q. Yin, Y.-X. Wang, Y. Zhang, J. Huang, H. Tan, Y. Yu, X. Li, L. Xu and H.-B. Yang, *Nat. Commun.*, 2018, **9**, 3190; (*c*) X.-Q. Wang, W.-J. Li, W. Wang, J. Wen, Y. Zhang, H. Tan and H.-B. Yang, *J. Am. Chem. Soc.*, 2019, **141**, 13923–13930; (*d*) W.-J. Li, X.-Q. Wang, W. Wang, Z. Hu, Y. Ke, H. Jiang, C. He, X. Wang, Y.-X. Hu, P.-P. Jia, P. Yin, J. Chen, H. Sun, Z. Sun, L. Xu and H.-B. Yang, *Giant*, 2020, **2**, 100020; (*e*) W.-J. Li, W. Wang, X.-Q. Wang, M. Li, Y. Ke, R. Yao, J. Wen, G.-Q. Yin, B. Jiang, X. Li, P. Yin and H.-B. Yang, *J. Am. Chem. Soc.*, 2020, **142**, 8473–8482; (*f*) W.-J. Li, Z. Hu, L. Xu, X.-Q. Wang, W. Wang, G.-Q. Yin, D.-Y. Zhang, Z. Sun, X. Li, H. Sun and H.-B. Yang, *J. Am. Chem. Soc.*, 2020, **142**, 16748–16756; (*g*) W.-J. Li, W.-T. Xu, X.-Q. Wang, Y. f. Jiang, Y. Zhu, D.-Y. Zhang, X.-Q. Xu, L.-R. Hu, W. Wang and H.-B. Yang, *J. Am. Chem. Soc.*, 2023, **145**, 14498–14509; (*h*) X.-Q. Wang, W.-J. Li, W. Wang and H.-B. Yang, *Acc. Chem. Res.*, 2021, **54**, 4091–4106; (*i*) Y. Zhu, H. Jiang, W. Wu, X.-Q. Xu, X.-Q. Wang, W.-J. Li, W.-T. Xu, G. Liu, Y. Ke, W. Wang and H.-B. Yang, *Nat. Commun.*, 2023, **14**, 5307; (*j*) X.-Q. Xu, W.-J. Li, D.-Y. Zhang, Y. Zhu, W.-T. Xu, Y. Wang, X.-Q. Wang, W. Wang and H.-B. Yang, *Angew. Chem., Int. Ed.*, 2025, **64**, e202419434.

21 (*a*) P. Hari and B. König, *Chem. Commun.*, 2014, **50**, 6688–6699; (*b*) Y. Kuang, K. Wang, X. Shi, X. Huang, E. Meggers and J. Wu, *Angew. Chem., Int. Ed.*, 2019, **58**, 16859–16863; (*c*) X.-Z. Fan, J.-W. Rong, H.-L. Wu, Q. Zhou, H.-P. Deng, J. D. Tan, C.-W. Xue, L.-Z. Wu, H.-R. Tao and J. Wu, *Angew. Chem., Int. Ed.*, 2018, **57**, 8514–8518; (*d*) J. Yan, H. Tang, E. J. R. Kuek, X. Shi, C. Liu, M. Zhang, J. L. Piper, S. Duan and J. Wu, *Nat. Commun.*, 2021, **12**, 7214; (*e*) P. Jia, Y. Hu, Z. Zeng, Y. Wang, B. Song, Y. Jiang, H. Sun, M. Wang, W. Qiu and L. Xu, *Chin. Chem. Lett.*, 2023, **34**, 107511.